Chemical Engineering Journal 156 (2010) 56–63

Contents lists available at ScienceDirect

Chemical Engineering Journal

journal homepage: www.elsevier.com/locate/cej

Removal of perchlorate from aqueous solution using protonated cross-linked chitosan

Yanhua Xie, Shiyu Li, Fei Wang, Guangli Liu*

School of Environmental Science and Engineering, Sun Yat-sen University, Guangzhou 510275, China

ARTICLE INFO

Article history:
Received 12 June 2009
Received in revised form
18 September 2009
Accepted 21 September 2009

Keywords:
Protonated cross-linked chitosan
Perchlorate
Adsorption
Regeneration

ABSTRACT

Protonated cross-linked chitosan was used to remove perchlorate from aqueous solution. Adsorption isotherms, the effects of pH and co-existing anions on the adsorption process, proper actual contact time in the adsorption column and the regeneration ability of the adsorbent were investigated. The equilibrium data fitted well with Langmuir and Freundlich isotherm models, and the maximum monolayer adsorption capacity was 45.455 mg g^{-1}. To balance the protonated degree of the amino groups and the effect of the ion competing on adsorption capacity, the optimal pH value was determined to be about 4.0. Column adsorption results indicated that the proper actual contact time was 8.1 min and the effluent perchlorate could be steadily kept below 24.5 μg L^{-1} up to about 95 bed volumes with the influent perchlorate of 10 mg L^{-1}. The presence of other anions weakened the perchlorate adsorption, especially the high valence anion such as sulfate. The adsorbents could be well regenerated by sodium hydroxide solution with pH 12 and reused at least for 15 cycles. Electrostatic attraction as well as physical force was the main driving force for perchlorate adsorption.

1. Introduction

Perchlorate (ClO_4^-) is commonly used in rocket propellant, explosives, missiles, pyrotechnics, air bags and other industries [1–4]. As an emergent environmental contaminant, perchlorate has been detected in soil, surface water as well as ground water. It has been shown to inhibit iodide uptake by the thyroid gland and disturb normal metabolism, which would retard physical and mental growth and lead to a series of diseases such as neurological damage and anemia [5]. Meanwhile, perchlorate can be stable existing in the normal environment for several decades due to its characteristics of high solubility, non-reactivity, and poor adsorption by soil [6–8]. In order to prevent the health risk from perchlorate pollution, the USEPA set a Drinking Water Equivalent Level (DWEL) of 24.5 μg L^{-1} in 2005 [9].

The main treatment technologies for perchlorate are as follows: (1) ion exchange (IX) [10,11], (2) biological treatment [12,13], (3) adsorption by activated carbon (AC) or tailored AC [14–16], and (4) others including membrane filtration [17], chemical/catalytic reduction and electrochemical reduction [18–20]. Biological treatment is cost-effective for seriously contaminated water with high perchlorate concentration, organics, co-contaminants, and suspended solids, but it is costly for perchlorate contaminated water with finite concentration. Furthermore, it requires subsequent disposal of the added nutrients and microorganisms from the treated water [1,21]. Ion exchange is one of the most promising methods to remove low level of perchlorate at a high flow rate [22]. However, the high cost for resin regeneration and regenerant disposal would inhibit its wide use unless the two issues could be resolved [23,24]. AC is more favored for adsorbing non-polar pollutants with low water solubility in most cases and unfavorable for adsorbing perchlorate, so it always needs to be tailored or modified [14–16].

Recently, great attention has been paid to the natural biosorbent of chitosan, which is derived from thermo-chemical deacetylation of polysaccharide chitin. Chitosan has the properties of high hydrophilicity, non-toxicity, and biodegradability. Moreover, it is abundant in nature [25,26]. It has been widely used to remove heavy metals [26–28], organic contaminants, such as chlorophenols, humic acids, dyes and colors [29–31], and some anions [32–34] due to its high content of amino ($-NH_2$) and hydroxy ($-OH$) functional groups, which have high activity as adsorption sites. However, there has been no report about using chitosan to remove perchlorate as far as we know. As chitosan flakes or powder is less stable and difficult to be separated after adsorption, it needs to be modified into a stable form before effective use. In addition, the free $-NH_2$ groups in chitosan would be protonated and become into $-NH_3^+$, which shows greater tendency to absorb anions. So protonated cross-linked chitosan was employed to remove perchlorate from water in the present work. Batch and column experiments

* Corresponding author. Tel.: +86 20 84112293; fax: +86 20 84110267.
E-mail address: liugl@mail.sysu.edu.cn (G. Liu).

1385-8947/$ – see front matter © 2009 Elsevier B.V. All rights reserved.
doi:10.1016/j.cej.2009.09.033

were conducted to evaluate the adsorption capability and to determine the regeneration feasibility of the adsorbent.

2. Materials and methods

2.1. Materials

Chitosan powder (deacetylation degree is greater than 95%, viscosity is 150 mPa s) was acquired from Golden-shell Biochemical Co. (Zhejiang, China). All reagents used in this study, including $NaClO_4 \cdot H_2O$, $NaNO_3$, Na_2SO_4, HCl, NaOH, acetic acid and glutaraldehyde, were of analytical grade supplied by Guangzhou Chemical Reagent Factory, China. Aqueous solutions were prepared using deionized water with a resistance of 18 MΩ cm obtained from a Millipore filtering system.

2.2. Preparation of cross-linked and protonated cross-linked chitosan beads

Chitosan powder was dissolved into 2% (v/v) acetic acid and made into 2.5 wt.% solution. The solution was completely dissolved and de-bubbled after 1 h standing reaction. The homogeneous solution was then injected into a plastic beaker containing a 2 M sodium hydroxide solution through a hypodermic needle. As a result, highly porous, milky white spherical gel beads formed and settled at the bottom of the container. After gelling for 6 h in sodium hydroxide solution, the beads were separated by a sieve with the pore size of 1 mm and washed with distilled water repeatedly to reach neutrality. The neutral beads were dipped into a 20% glutaraldehyde solution with gentle mixing in a shaking incubator. Thus the cross-linked chitosan beads were obtained after 24 h residence time. The beads were then washed with distilled water again to clean the residual glutaraldehyde, dried at 50 °C for 72 h, and sealed to storage in constant temperature in a humidity box [32]. The average diameter of the beads was about 1.5 mm with pure chitosan content about 67.934 mg g^{-1} beads under these conditions.

The cross-linked beads were protonated for 1 h in a given concentration of hydrochloric acid solution before each test with stirring in a shaking incubator at 150 rpm and 25 ± 1 °C in order to effectively utilize the amino groups of the chitosan for perchlorate adsorption. The concentrations of the hydrochloric acid solutions were determined by the demanded pH of the adsorption runs [32]. The protonated cross-linked chitosan beads were directly used to adsorb perchlorate without re-drying.

2.3. Analysis methods

Ion chromatography (IC) system (ICS 3000, Dionex) was used to determine the concentrations of perchlorate, chloride, nitrate and sulfate. All samples were filtrated with a 0.22 μm filter before measurement. The IC system was equipped with a set of 2 mm × 250 mm AS19 column and guard column, a 2-mm ASRS suppressor, an electrical conductivity detector, and an autosampler. The concentration of sodium hydroxide eluent was set to 50 mM for the perchlorate detection and 15 mM for the chloride, nitrate and sulfate analysis respectively. With the injection loop of 250 μL, the detection limit was 5 μg L^{-1} for perchlorate, and 2 μg L^{-1} for chloride, nitrate and sulfate.

2.4. Adsorption experiments

2.4.1. Batch experiments

Duplicate batch experiments were conducted to investigate the effect of pH and competing anions on perchlorate adsorption as well as adsorption equilibrium isotherm. About 1 g of cross-linked chitosan beads were protonated and added into 100 mL of 10 mg L^{-1} perchlorate solution with desired pH values and competing anion concentrations. Equilibrium isotherm was determined by keeping the solution volume and the amount of the adsorbent constant and varying the concentration of perchlorate. The pH of the solution was adjusted by adding 1.0 M hydrochloric acid or 0.1 M sodium hydroxide. The pH was measured using a FE20K pH meter (Mettler Toledo, Switzerland). The solutions were mixed in a shaking incubator at a speed of 150 rpm and a constant temperature at 25 ± 1 °C. Although preliminary experiments showed that the adsorption equilibrium was almost reached in about 3 h, 24 h reaction time was kept to obtain the complete equilibrium. After the reaction finished, 10 mL sample was taken by using a single injector, and filtrated before it was analyzed by IC system. The amount of adsorption per unit mass of chitosan at equilibrium, q_e (mg g^{-1}) was calculated by the following equation

$$q_e = \frac{(C_0 - C_e)V}{W} \quad (1)$$

where C_0 and C_e are initial and equilibrium concentrations of perchlorate (mg L^{-1}) respectively, W is dry mass of chitosan present in 1 g of cross-linked chitosan bead (67.934 mg chitosan/g bead), and V is solution volume (L).

Table 1
Conditions of the column tests for adsorption ClO_4^- onto protonated cross-linked chitosan.

Flow rate (mL min^{-1})	EBCT[a] (min)	ART[b] (min)
0.8	31.2	12.2
1.1	22.7	8.1
1.6	15.6	5.3
3.5	7.1	3.2

[a] The empty bed contact time, EBCT = the bed volume/the flow rate.
[b] The actual retention time, ART, measured actually.

2.4.2. Column experiments

Column adsorption experiments were used to investigate the breakthrough curves with different retention times and the effect of the competing anions on adsorption process. The experiments were conducted in a series of glass columns, which was 45 cm in length and 1 cm in diameter. The effective bed volume (BV) was 25 cm^3. About 14 g cross-linked chitosan beads were protonated and packed into each column. All the tests were carried out at a constant room temperature at 26 ± 2 °C. The influent solution was pumped through the column adopted up-flow mode in order to accurately control contact time and avoid channeling in the column. The desired empty bed contact time (EBCT) and actual retention time (ART) were listed in Table 1. The pH of influent solution was adjusted to 4.0 by adding hydrochloric acid. The samples of the effluent from each column were collected at certain time intervals and monitored by IC. Each test was continuously run until the column was significantly broken through.

2.5. Regeneration and reuse ability of the absorbents

Batch tests were conducted to investigate the necessary regeneration time at first. The exhausted absorbent was collected from the equilibrium test with an initial perchlorate concentration of 10 mg L^{-1} and transferred into a clean conical bottle containing 100 mL sodium hydroxide solution with pH 12. Then the mixture was agitated at a speed of 150 rpm and a constant temperature at 25 ± 1 °C. Samples were collected at given time intervals and measured by IC. Fifteen cycles of protonation–adsorption–regeneration were repeated under the same conditions in order to investigate the reuse ability of the absorbents.

In column test, when the column was significantly broken through by perchlorate, the residual solution in the column was

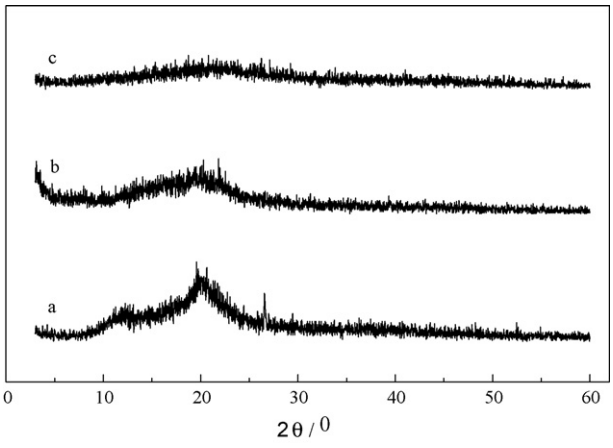

Fig. 1. X-ray diffraction profiles of chitosan: (a) virgin chitosan; (b) cross-linked chitosan; (c) protonated cross-linked chitosan.

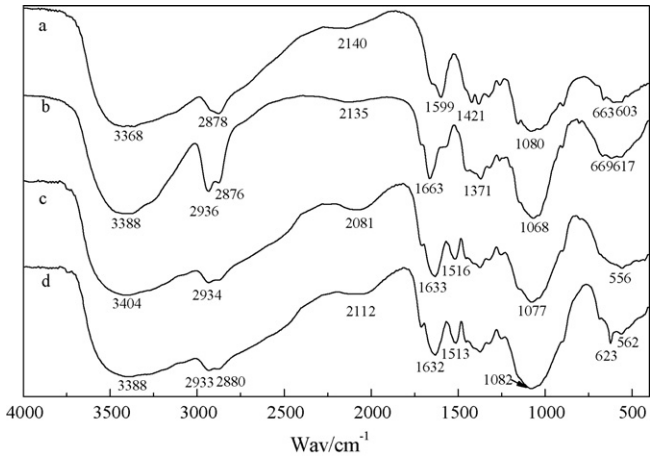

Fig. 2. FTIR spectra of chitosan: (a) virgin chitosan; (b) cross-linked chitosan; (c) protonated cross-linked chitosan; (d) protonated cross-linked chitosan loaded with ClO_4^-.

drained by pumping in air. Then hydroxide solution with pH 12 was pumped into the column at a constant flow rate of 1.2 mL min^{-1} (according to the results of the batch test described above). Samples of perchlorate were collected at certain time intervals and monitored by IC as well. When the effluent concentration of perchlorate was undetectable, it was assumed that regeneration process was completed.

2.6. Characterizations of the adsorbent

X-ray diffraction (XRD) profiles of virgin chitosan, cross-linked chitosan, as well as protonated cross-linked chitosan were characterized by a RIGAKUD/max–IIIA of Powder X-ray Diffractometer (Japan) with diffraction angle (2θ) ranging from 3° to 60° to observe the crystal structure transformation of the adsorbents during the modification process. Besides, Fourier-transform infrared (FTIR) spectra of the chitosan samples were also recorded with EQUINOX 55 Fourier Transformation Infra-red Spectrometer coupled with Infra-red Microscope (Bruker, Germany) using KBr pellets prepared by mixing the chitosan power with KBr. The spectra of FTIR could describe the changes of the functional groups presented in chitosan during the modification process and after perchlorate being adsorption.

3. Results and discussion

3.1. Characterization of adsorbents

3.1.1. X-ray diffraction

XRD profiles of virgin chitosan, cross-linked chitosan, and protonated cross-linked chitosan are shown in Fig. 1. The 12° (broad peak), 20° (broad peak) and 26° of 2θ are the natural crystal peaks of virgin chitosan expressed by "curve a" in Fig. 1. After being cross-linked by sodium hydroxide and glutaraldehyde ("curve b" in Fig. 1), the intensity of the natural crystal peaks weakened obviously. Furthermore, the peaks nearly disappeared when protonated by hydrochloric acid ("curve c" in Fig. 1). The results indicated that the action forces of hydrogen bonds among molecules were weakened through the modified process, and the crystal structure of the chitosan became much more disordered, making the amine groups in the chitosan more accessible for adsorption. So the modified chitosan with lower crystal energy is more prone to react with other substances than the virgin chitosan [38].

3.1.2. Fourier-transform infrared spectra

FTIR spectra expressed in Fig. 2 were conducted to observe the transmutation of the functional groups in chitosan molecule during the modification and adsorption process in detail. The spectrum of the virgin chitosan was a standard chitosan spectrum in free amino form described by "curve a" in Fig. 2. A broad peak appears at the range of 3500–3200 cm^{-1} attributing to O–H and N–H stretching vibrations, while the peaks at 2878, 2140, and 1080 cm^{-1} are due to C–H, C–NH_2, and C–O stretching vibrations respectively [38,39]. The main amine and amide bands on chitosan are as follows: Amide I, C–O stretching band conjugated with N–H deformation band at 1650 cm^{-1}; Amide II, N–H and C=N deformation bands ranging from 1550 to 1590 cm^{-1}; Amide III, N–H deformation band conjugated with C=O and C=N stretching bands at about 1300 cm^{-1}; Amine bands including –NH_2 free amine at 1605–1580 cm^{-1} and –NH_3^+ at 1550–1480 cm^{-1} [40]. According to "curve a" in Fig. 2, the prominent band was observed at 1599 cm^{-1} corresponding to the free amine form of glucosamine residues. The amide I (1650 cm^{-1}) and amide II (1550–1590 cm^{-1}) bands were very weak due to high deacetylation degree of chitosan used in this research.

The spectrum of cross-linked chitosan is shown by "curve b" in Fig. 2. The most important peak in this region appeared near 1663 cm^{-1} attributing to –C=N– (Schiff alkali) band [40]. The form of Schiff alkali could protect the –NH_2 functions on chitosan and prevent the chitosan from dissolving in strong acid during the following protonation process. Meanwhile, the band of free amine functions almost disappeared owing to a high level of consumption during the cross-linking reaction.

"Curve c" in Fig. 2 shows the spectrum of protonated cross-linked chitosan. The –C=N– band greatly weakened and was covered up by a new peak of N–H_2 shear deformation vibration appearing at 1633 cm^{-1}. Besides, two new important bands of $RNH_3^+Cl^-$ and –NH_3^+ appeared near 2081 and 1516 cm^{-1} respectively [41,42]. The transformation of the functional groups indicated that the –NH_2 group on chitosan was protonated and became –NH_3^+ and $RNH_3^+Cl^-$ in an acidic medium which is favorable for anion adsorption.

3.2. Effect of pH

The adsorption of perchlorate onto chitosan is highly dependent on the pH of the solution, which affects the surface charge of the chitosan. Report has shown that the pH_{zpc} (pH at which the surface has a net zero charge) of chitosan is 6.3 [26]. When the pH is less than pH_{zpc}, the net surface charge on the chitosan becomes pos-

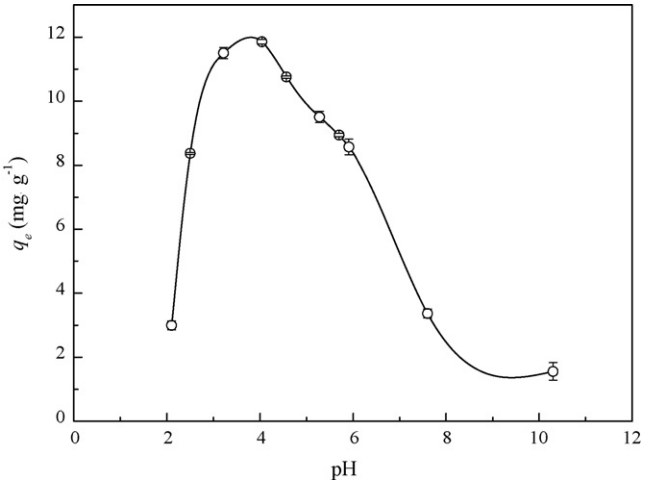

Fig. 3. Effect of pH on adsorption of ClO_4^- onto protonated cross-linked chitosan. Initial ClO_4^- = 10 mg L^{-1}.

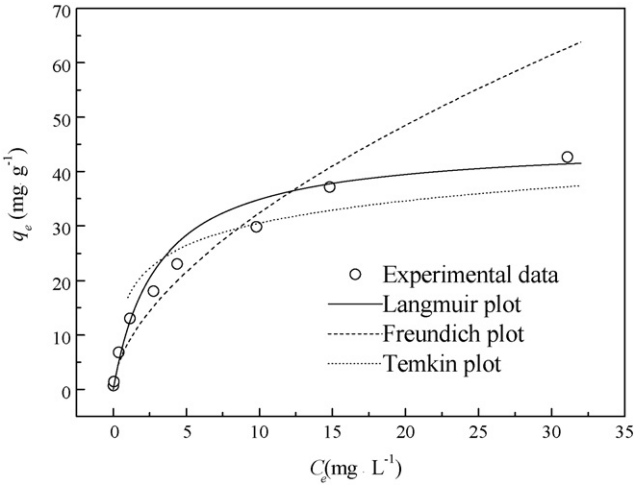

Fig. 4. Isotherm plots for the adsorption of ClO_4^- onto protonated cross-linked chitosan. pH 4.0.

itive as the $-NH_2$ is protonated and becomes $-NH_3^+$ in an acidic medium. In addition, almost 90% of total amine groups of the chitosan are protonated when the pH is below 5 [33,34]. Generally the increasing electrostatic interactions between the negatively charged perchlorate and positively charged amine groups of chitosan cause an increase in the perchlorate adsorption at lower pH [34].

The variation of adsorption capacity of the cross-linked protonated chitosan with pH for perchlorate is presented in Fig. 3. The plots indicate that the maximum adsorption capacity was reached at pH 4.0. When the pH further decreased, even more protons could be got and used to $-NH_2$ protonation, the adsorption capacity of the adsorbent decreased sharply and was very weak at pH 2.1. The reason may be that excessive chloride ions would compete with perchlorate to occupy the adsorption sites in the adsorbent or the adsorbent structure was damaged at very low pH condition. The exhausted chitosan beads at pH 2.1 were regenerated using sodium hydroxide with pH 12 and reused to adsorb perchlorate at pH 4.0 to clear this phenomenon. If it was just because of ion competing, the reused adsorbent could recover its adsorption capability. If there was breakage in the adsorbent structure, the adsorption efficiency of the reused adsorbent was irreversible. The results showed that the adsorption capability of the reused adsorbent was close to the virgin adsorbent, indicating that there was no breakage of the adsorbent structure. So ion competing at low pH may be the main reason for weakening the adsorption capability of the adsorbent.

The positive surface charge of chitosan gradually decreases with increasing in pH and has zero potential at pH 6.3 as fewer protons exist in solution. As a result, the decreasing electrostatic interaction between the perchlorate and the amine groups of chitosan results in less adsorption capability with pH increasing. However, at pH 7.6, where the surface charge of chitosan beads was neutral, the amount of perchlorate adsorption by the adsorbent indicated that physical forces might be another driven force for perchlorate adsorption. When the pH increased up to 10.3, the adsorption amount was very weak, so it greatly facilitated the regeneration of the adsorbent. Therefore, pH 4.0 was recognized as the optimal value considering the protonated degree of amino groups in chitosan and the effect of ion competing on adsorption capacity.

3.3. Adsorption equilibrium isotherms

Adsorption isotherm is helpful for understanding how adsorbate interacts with adsorbent. Preliminary experiments showed that the q_e were 12.074 ± 0.107, 11.853 ± 0.074 and 11.741 ± 0.043 mg g^{-1} respectively corresponding to the temperature of 15, 25 and 35 °C at the same reaction conditions, which indicates that the effect of temperature on perchlorate adsorption by the adsorbent was very limited. So the adsorption equilibrium isotherm study was just carried out at 25 ± 1 °C with the pH of 4.0. The equilibrium adsorption data were analyzed by using the linear form of Langmuir (Eq. (2)), Freundlich (Eq. (3)), and Tempkin (Eq. (4)) isotherm models [35–37] listed as follows:

$$\frac{C_e}{q_e} = \frac{1}{Q_0 b} + \frac{C_e}{Q_0} \quad (2)$$

$$lgq_e = lgK_f + \frac{1}{n} lgC_e \quad (3)$$

$$q_e = B \ln A + B \ln C_e \quad (4)$$

where C_e is the equilibrium concentration of perchlorate (mg L^{-1}), q_e is the amount of adsorption per unit mass of chitosan at equilibrium (mg g^{-1}), Q_0 (mg g^{-1}) and b (L mg^{-1}) are Langmuir constants reflected to the adsorption capacity and rate of adsorption corresponding to monolayer coverage; K_f and $1/n$ are Freundlich constants related to adsorption capability and adsorption intensity; A and B are Tempkin constants with $B = RT/b$. All of the constants can be calculated from the slopes and intercepts of the respective linear equations. The detail plots are depicted in Fig. 4, and the constant values of the three models along with regression coefficients (R^2) are listed in Table 2. The applicability of the isotherm to the adsorption was judged by comparing the values of R^2, which indicated that the equilibrium data were well fitted with the Langmuir (R^2 = 0.985) and Freundlich (R^2 = 0.962) isotherm models. The results revealed that the adsorption process was a combined process of homogeneous and heterogeneous adsorption, while the effects of indirect adsorbate and adsorbent interactions on adsorption process could be neglected. Thus the adsorption occurred mainly via the elec-

Table 2
Parameters of Langmuir, Freundlich and Tempkin isotherms for adsorption of ClO_4^- onto protonated cross-linked chitosan.

Adsorption model	Parameters		
Langmuir	Q_0 (mg g^{-1})	b (L mg^{-1})	R^2
	45.455	0.329	0.9852
Freundlich	K_F	$1/n$	R^2
	8.433	0.584	0.9616
Tempkin	A (L g^{-1})	B	R^2
	17.249	5.919	0.9207

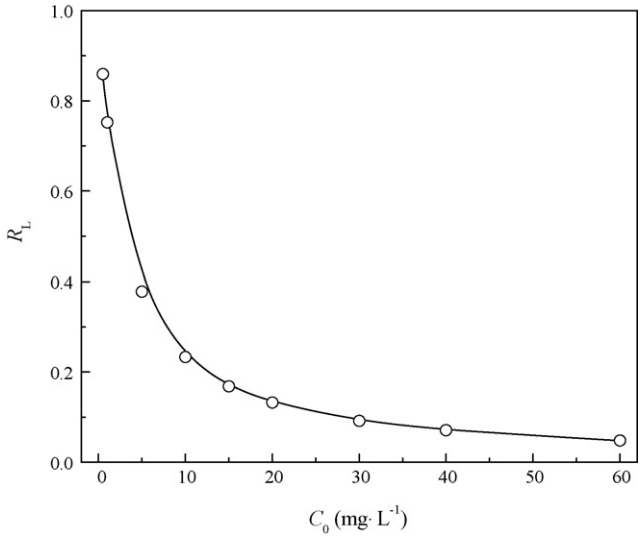

Fig. 5. Equilibrium parameter (R_L) of Langmuir adsorption isotherm.

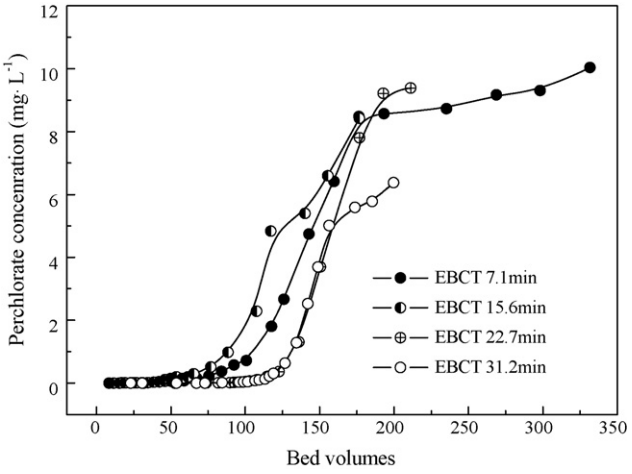

Fig. 6. Breakthrough curves for adsorption of ClO_4^- onto protonated cross-linked chitosan at different retention times. Influent concentration of ClO_4^- =10 mg L^{-1}; pH 4.0; and bed volume = 25 cm^3.

trostatic interactions between perchlorate anions and positively charged amino groups as well as physical forces. The results were consistent with the results expressed in the effect of pH.

The essential characteristics of the Langmuir isotherm model can be expressed by a dimensionless constant named equilibrium parameter R_L [36,37], which is defined as:

$$R_L = \frac{1}{1 + bC_0} \quad (5)$$

where b is the Langmuir constant (L mg^{-1}) and C_0 is the initial concentration of perchlorate (mg L^{-1}). R_L values express whether the adsorption is irreversible ($R_L = 0$), favorable ($0 < R_L < 1$), linear ($R_L = 1$), or unfavorable ($R_L > 1$). Fig. 5 shows the R_L values with the initial concentration of perchlorate from 0.5 to 60.0 mg L^{-1}. All of the R_L values were between 0 and 1, indicating that the adsorption of perchlorate on chitosan was favorable. The R_L values varied from 0.859 to 0.048 with the initial concentrations increased from 0.5 to 60.0 mg L^{-1}, which indicated that the adsorption was more favorable at higher initial concentration. In addition, the Freundlich constant of $1/n$ lying between 0 and 1, which further confirmed the favorable conditions for the adsorption [43].

3.4. Breakthrough curves in column adsorption experiments

The protonated cross-linked chitosan beads are usually packed into columns as ion exchange resins to facilitate the practical application. Different EBCT ranged from 7.1 to 31.2 min were conducted in column tests in order to determine the adequate reaction time of perchlorate with protonated cross-linked chitosan bead bed, and the breakthrough curves are shown in Fig. 6. The EDWEL of 24.5 μg L^{-1} set by USEPA was chosen as breakthrough point. With an influent concentration at 10 mg L^{-1}, the initial breakthrough points of perchlorate occurred at approximate 32, 38, 95 and 96 BVs corresponding with the EBCT of 7.1, 15.6, 22.7 and 31.2 min (the ART were 3.2, 5.3, 8.1, and 12.2 min) respectively. And the amounts of adsorption (q_e) were approximately 8.883, 10.094, 24.982, and 25.235 mg g^{-1} respectively. The results indicated that longer hydraulic retention time resulted in better adsorption efficiency. For example, the adsorption capacity doubled when the EBCT increased from 15.6 to 22.7 min. While there was no significant enhancement when further extended the retention time to 31.2 min. By considering the removal efficiency and operation cost synthetically, the EBCT of 22.7 min (ART 8.1 min) was the proper one.

3.5. Effect of competing anion

Nitrate and sulfate are common co-contaminants in perchlorate polluted water, and major competing ions adsorbed by the resin during water treatment process [23,24]. Both column and batch experiments were conducted to investigate the effect on adsorption from the nitrate and sulfate. Fig. 7 illustrates the breakthrough curves of nitrate, sulfate and perchlorate from the protonated cross-linked chitosan bead bed by keeping 10 mg L^{-1} as the initial concentration with pH 4.0. The plots show that the protonated cross-linked chitosan favorably adsorbed the anions in the following order: sulfate > perchlorate > nitrate. For example, the effluent concentrations of nitrate, perchlorate and sulfate were 10.195, 1.075, and 0.137 mg L^{-1} respectively at 29 BVs when nitrate was completely broken through. The peak at 37 BVs on the nitrate breakthrough curve further demonstrated the preferential adsorption of sulfate and perchlorate compared to nitrate. The breakthrough point of perchlorate was at 15 BVs that was much shorter than that without competing ions (breakthrough point at

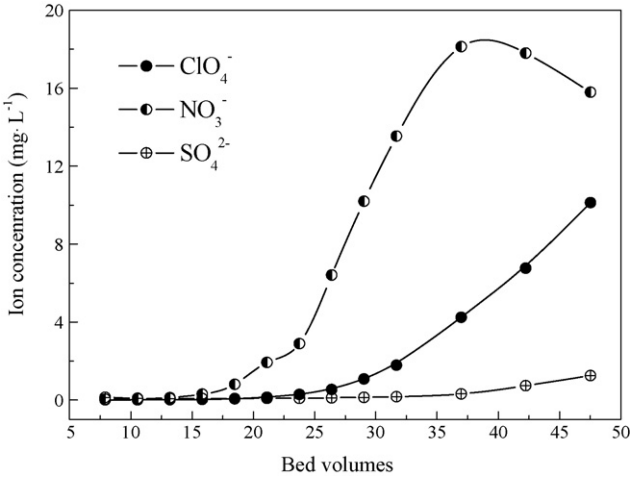

Fig. 7. Breakthrough curves for adsorption of NO_3^-, ClO_4^- and SO_4^{2-} onto protonated cross-linked chitosan. EBCT = 22.7 min, influent concentration = 10 mg L^{-1}; pH 4.0; and bed volume = 25 cm^3.

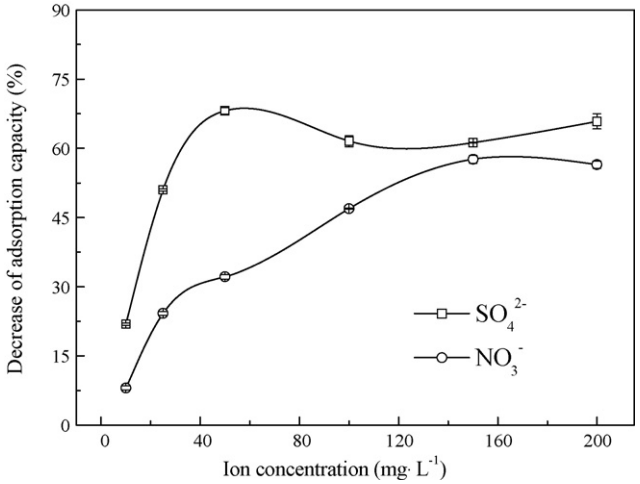

Fig. 8. Effects of NO_3^- and SO_4^{2-} on the adsorption capacity of ClO_4^- onto protonated cross-linked chitosan. Batch tests, concentration of ClO_4^- = 10 mg L^{-1}; pH 4.0; the concentration of NO_3^- and SO_4^{2-} range from 10 mg L^{-1} to 200 mg L^{-1}.

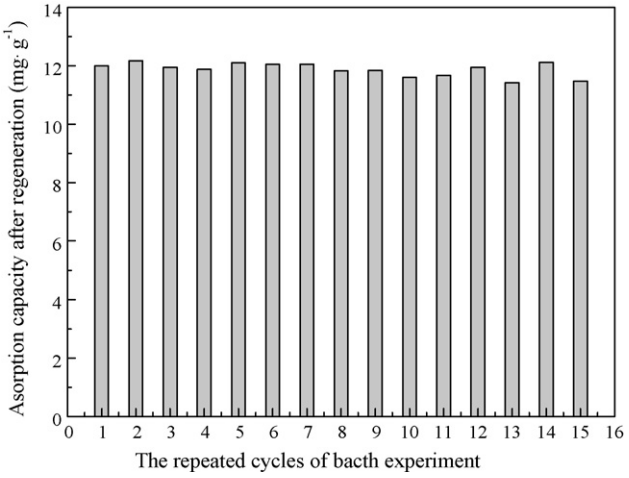

Fig. 10. Recovery of protonated cross-linked chitosan adsorption capacity to ClO_4^- in 15 repeated loading and regeneration cycles. Batch tests, initial ClO_4^- concentration = 10 mg L^{-1}; pH 4.0; the pH of regeneration NaOH solution = 12.

95 BVs). Batch tests also show that sulfate has a much greater influence on perchlorate adsorption onto chitosan than comparable level of nitrate (Fig. 8). With the concentration increase of the competing anions, a reduction adsorption of perchlorate was observed. For instance, when the concentration of sulfate varied from 10 to 50 mg L^{-1}, the adsorption capability decreased by 21–68% respectively. In brief, in the presence of other anions, there was a competition among them for the adsorption sites on the adsorbent surfaces, resulting in less perchlorate adsorption, especially for high valence anions such as sulfate.

3.6. Regeneration and reuse ability

About 73% of the adsorption capacity could be recovered during the batch regeneration process within 5 min, so the EBCT of 20.8 min (ART was 7.4 min) with 1.2 mL min^{-1} flow rate was determined in regeneration column tests. The regeneration curve of the spent bead bed by using sodium hydroxide solution with pH 12 is illustrated in elution profile of perchlorate (Fig. 9). The plots indicate that the adsorbed perchlorate could be rapidly eluted and concentrated within 3 BVs of the regeneration solution. The eluted perchlorate was highly concentrated around 2.4 BVs in regeneration solution with the concentration up to 729 mg L^{-1}, which greatly facilitates the subsequent perchlorate destruction. The adsorption sites of protonated cross-linked chitosan beads could be completely recovered within 15 BVs of the eluent.

Fig. 10 shows that after proper regeneration for 15 cycles, the adsorption efficiency of perchlorate onto protonated cross-linked chitosan beads had no significant decrease. The results indicated that the adsorbent loaded with perchlorate could be regenerated effectively by sodium hydroxide solution with pH 12, and the adsorbent had good performance for repeated use.

3.7. Adsorption mechanism

"Curve d" in Fig. 2 illustrates the profile of protonated cross-linked chitosan loaded with perchlorate. Compared with "curve c" in Fig. 2, the intensity of $-NH_3^+$ band at 1513 cm^{-1} was not significantly changed, while the intensity of $RNH_3^+Cl^-$ band at 2112 cm^{-1} weakened slightly. Besides, it is worthy noting that a new acuti-peak occurred at 623 cm^{-1}. One of the characteristic bands of perchlorate is just between 650 and 600 cm^{-1} [42], which indicates that the perchlorate anions were adsorbed onto the adsorbent surface. The above observation showed that the adsorption process of perchlorate onto chitosan in acidic solution might be achieved through electrostatic attraction between positively

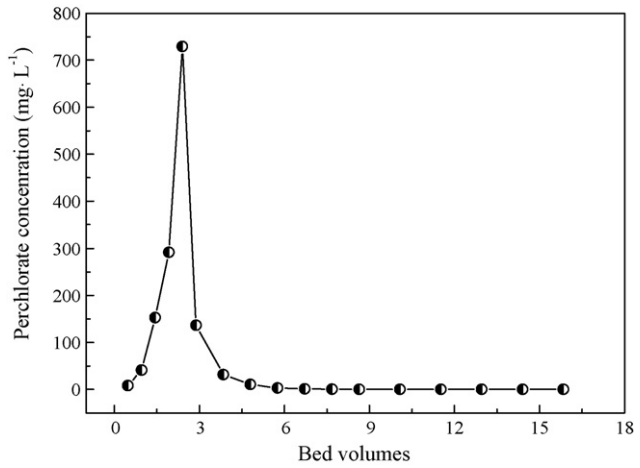

Fig. 9. Regeneration of protonated cross-linked chitosan bead bed exhausted with ClO_4^- using pH 12 NaOH. EBCT = 20.8 min, bed volume = 25 cm^3.

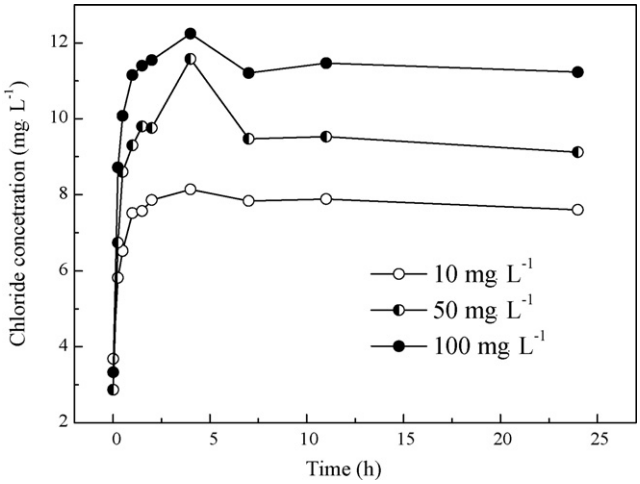

Fig. 11. Change of chloride concentration in solution during the adsorption process. Batch tests, initial perchlorate concentrations were 10, 50 and 100 mg L^{-1}; pH 4.0.

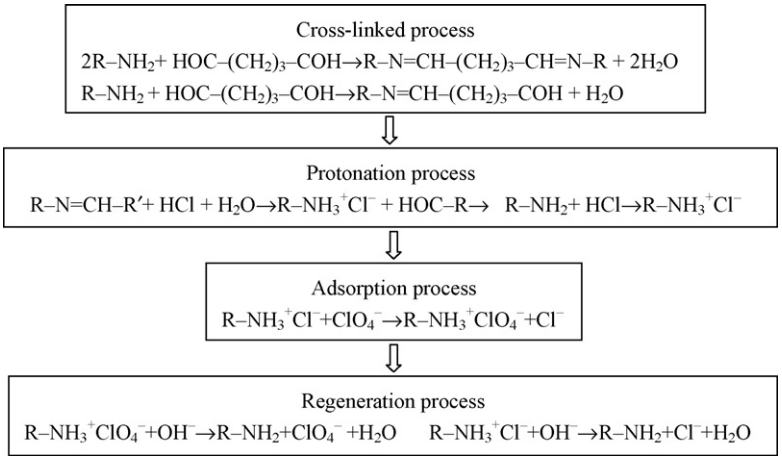

Scheme 1. Mechanism of adsorption ClO_4^- onto protonated cross-linked chitosan in acidic medium and its regeneration.

charged chitosan surfaces and negatively charged perchlorate ions. In addition, the variation of chloride concentration in solution was monitored for 24 h in batch tests during the adsorption process at three different initial perchlorate concentrations, viz. 10, 50 and 100 mg L^{-1}. The results are presented in Fig. 11, which indicate that the chloride concentration in the solution increased considerably at early adsorption stage (about 4 h), and then decreased slightly. It means that the main interaction between perchlorate anions and protonated sites of the adsorbent may have occurred through ion exchange of chloride with perchlorate during the adsorption process leading to the increasing of chloride in solution. After adsorption equilibrium was reached, few chloride anions would be re-adsorbed on the residual adsorption sites of the adsorbents, resulting in a slight decrease of chloride. Through material balance, the molar quantity of the chloride released into the solution was a little more than the perchlorate adsorbed by the adsorbents, suggesting that the perchlorate adsorption implemented mainly through ion exchange in acidic solution. A chloride balance was also observed during the protonation–adsorption–regeneration process. Furthermore, this phenomenon was more obvious at higher initial perchlorate concentrations because more chloride anions were exchanged from the absorbents. The mechanism of perchlorate removal by protonated cross-linked chitosan in acidic solution is briefly shown in Scheme 1.

It is worth noting that the cross-linked chitosan beads still had adsorption ability when the surface charge of the adsorbent was neutral and there was no electrostatic interaction between the perchlorate anions and the amine groups of the chitosan. So the amount of perchlorate adsorption by the adsorbents at neutral pH condition suggested that physical forces may be another driving force for perchlorate adsorption.

4. Conclusions

Through cross-linked and protonated modifications, chitosan was used for perchlorate removal from aqueous solution. Batch and column experiments were conducted to investigate the adsorption capability and the regeneration feasibility of the adsorbent. XRD and FTIR analysis showed that the modified adsorbents with lower crystal energy and protonated amino groups were favorable for anion adsorption. Considering the protonated degree of the amino groups in chitosan and the ion competing effect on adsorption capacity of chloride, pH 4.0 was chosen as the optimal value. The equilibrium data fitted well with Langmuir and Freundlich isotherm models, and the maximum monolayer adsorption capacity was 45.455 mg g^{-1}. In addition, the constant values of R_L and $1/n$ indicated that the adsorption of perchlorate was favorable. In column tests, the proper actual contact time was 8.1 min (EBCT 22.7 min) with the treatment capacity being 95 BVs and the adsorption amount of perchlorate being 24.982 mg g^{-1} approximately. The presence of competing anions resulted in less perchlorate adsorption, especially to high valence anion such as sulfate. Sodium hydroxide solution with pH 12 was found to be capable of recovering the column bed and the adsorbents could be reused at least for 15 cycles. So the adsorbent has good performance for repeated use. Electrostatic attraction and physical forces were the main driving forces for perchlorate adsorption. The results indicate that the bio-adsorbent of chitosan with cationic modification has a potential for application to perchlorate removal from contaminated water.

Acknowledgements

This work was partially supported by grants from the Research Fund Program of Sun Yat-sen University, the Natural Science Foundation of China (no. 50608070).

References

[1] E.T. Urbansky, M.R. Schock, Issues in managing the risks associated with perchlorate in drinking water, J. Hazard. Mater. 56 (1999) 79–95.
[2] Y.C. Choia, X. Lic, L. Raskinc, E. Morgenroth, Chemisorption of oxygen onto activated carbon can enhance the stability of biological perchlorate reduction in fixed bed biofilm reactors, Water Res. 42 (2008) 3425–3434.
[3] G.S. Lehman, M. Badruzzamanc, S. Adham, D.J. Roberts, D.A. Clifford, Perchlorate and nitrate treatment by ion exchange integrated with biological brine treatment, Water Res. 42 (2008) 969–976.
[4] S.W. Van Ginkel, C.H. Ahn, M. Badruzzaman, D.J. Roberts, S.G. Lehman, S.S. Adham, B.E. Rittmann, Kinetics of nitrate and perchlorate reduction in ion-exchange brine using the membrane biofilm reactor (MBfR), Water Res. 42 (2008) 4197–4205.
[5] F.X. Li, L. Squartsoff, S.H. Lamm, Prevalence of thyroid deseases in Nevada counties with respect to perchlorate in drinking water, J. Occup. Environ. Med. 43 (2001) 630–634.
[6] B.E. Logan, Assessing the outlook for perchlorate remediation, Environ. Sci. Technol. 35 (2001) 482A–487A.
[7] B.H. Gu, W.J. Dong, G.M. Brown, D.R. Cole, Complete degradation of perchlorate in ferric chloride and hydrochloric acid under controlled temperature and pressure, Environ. Sci. Technol. 37 (2003) 2291–2295.
[8] H.P. Huq, J.S. Yang, J.W. Yang, Removal of perchlorate from groundwater by the polyelectolyte-enhanced ultrafiltration process, Desalination 204 (2007) 335–343.
[9] C. Wang, L. Lippincott, X.G. Meng, Feasibility and kinetics study on the direct bio-regeneration of perchlorate laden anion-exchange resin, Water Res. 42 (2008) 4619–4628.
[10] P.V. Bonnesen, G.M. Brown, S.D. Alexandratos, L. Bates Bavoux, D.J. Presley, V. Patel, R. Ober, B.A. Moyer, Development of bifunctional anion-exchange resins with improved selectivity and sorptive kinetics for pertechnetate: batch-equilibrium experiments, Environ. Sci. Technol. 34 (2000) 3761–3766.
[11] Z. Xiong, D. Zhao, G. Pan, Rapid and complete destruction of perchlorate in water and ion-exchange brine using stabilized zero-valent iron nanoparticles, Water Res. 41 (2007) 3497–3505.

[12] B.E. Logan, J. Wu, R.F. Unz, Biological perchlorate reduction in high-salinity solutions, Water Res. 35 (2001) 3034–3038.
[13] A. Patel, G. Zuo, S.G. Lehman, M. Badruzzaman, D.A. Clifford, D.J. Roberts, Fluidized bed reactor for the biological treatment of ion-exchange brine containing perchlorate and nitrate, Water Res. 42 (2008) 4291–4298.
[14] W. Chen, F.S. Cannon, J.R. Rangel-Mendez, Ammonia-tailoring of GAC to enhance perchlorate removal. I: characterization of NH_3 thermally tailored GACs, Carbon 43 (2005) 573–580.
[15] W. Chen, F.S. Cannon, J.R. Rangel-Mendez, Ammonia-tailoring of GAC to enhance perchlorate removal. II: perchlorate adsorption, Carbon 43 (2005) 581–590.
[16] R. Parette, F.S. Cannon, The removal of perchlorate from groundwater by activated carbon tailored with cationic surfactants, Water Res. 39 (2005) 4020–4028.
[17] J. Yoon, Y. Yoon, G. Amy, J. Cho, D. Foss, T. Hyung, Use of surfactant modified ultrafiltration for perchlorate (ClO_4^-) removal, Water Res. 37 (2003) 2001–2012.
[18] A.M. Moore, C.H. De Leon, T.M. Young, Rate and extent of aqueous perchlorate removal by iron surfaces, Environ. Sci. Technol. 37 (2003) 3189–3198.
[19] K.D. Hurley, J.R. Shapley, Efficient heterogeneous catalytic reduction of perchlorate in water, Environ. Sci. Technol. 41 (2007) 2044–2049.
[20] D.M. Wang, C.P. Huang, Electrodialytically assisted catalytic reduction (EDACR) of perchlorate in dilute aqueous solutions, Sep. Purif. Technol. 59 (2008) 333–341.
[21] I.H. Yoon, X. Meng, C. Wang, K.W. Kim, S. Bang, E. Choe, L. Lippincott, Perchlorate adsorption and desorption on activated carbon and anion exchange resin, J. Hazard. Mater. 164 (2009) 87–94.
[22] B.H. Gu, Y.K. Ku, G.M. Brown, Sorption and desorption of perchlorate and U (VI) by strong-base anion-exchange resins, Environ. Sci. Technol. 39 (2005) 901–907.
[23] B.H. Gu, G.M. Brown, L. Maya, M.J. Lance, B.A. Moyer, Regeneration of perchlorate (ClO_4^-)-loaded anion exchange resins by a novel tetrachloroferrate ($FeClO_4^-$) displacement technique, Environ. Sci. Technol. 35 (2001) 3363–3368.
[24] B.H. Gu, G.M. Brown, C.C. Chiang, Treatment of perchlorate contaminated groundwater using highly selective, regenerable ion-exchange technologies, Environ. Sci. Technol. 41 (2007) 6277–6282.
[25] V.M. Boddu, K. Abburi, J.L. Talbott, E.D. Smith, Removal of hexavalent chromium from wastewater using a new composite chitosan biosorbent, Environ. Sci. Technol. 37 (2003) 4449–4456.
[26] V.M. Boddu, K. Abburi, J.L. Talbott, E.D. Smith, R. Haasch, Removal of arsenic (III) and arsenic (V) from aqueous medium using chitosan-coated biosorbent, Water Res. 42 (2008) 633–642.
[27] Y.A. Aydın, N.D. Aksoy, Adsorption of chromium on chitosan: optimization, kinetics and thermodynamics, Chem. Eng. J. 151 (2009) 188–194.
[28] W.L. Yan, R. Bai, Adsorption of lead and humic acid on chitosan hydrogel beads, Water Res. 39 (2005) 688–698.
[29] F.C. Wu, R.L. Tseng, R.S. Juang, Enhanced abilities of highly swollen chitosan beads for color removal and tyrosinase immobilization, J. Hazard. Mater. B81 (2001), pp. 167-77.
[30] S. Bratskaya, S. Schwarz, D. Chervonetsky, Comparative study of humic acids flocculation with chitosan hydrochloride and chitosan glutamate, Water Res. 38 (2004) 2955–2961.
[31] S. Zheng, Z. Yang, D.H. Jo, Y.H. Park, Removal of chlorophenols from groundwater by chitosan sorption, Water Res. 38 (2004) 2315–2322.
[32] K. Jaafari, T. Ruiz, S. Elmaleh, J. Coma, K. Benkhouja, Simulation of a fixed bed adsorber packed with protonated cross-linked chitosan gel beads to remove nitrate from contaminated water, Chem. Eng. J. 99 (2004) 153–160.
[33] S. Chatterjee, S.H. Woo, The removal of nitrate from aqueous solutions by chitosan hydrogel beads, J. Hazard. Mater. 164 (2009) 1012–1018.
[34] S. Chatterjee, D.S. Lee, M.W. Lee, S.H. Woo, Nitrate removal from aqueous solutions by cross-linked chitosan beads conditioned with sodium bisulfate, J. Hazard. Mater. 166 (2009) 508–513.
[35] D. Kavitha, C. Namasivayam, Experimental and kinetic studies on methylene blue adsorption by coir pith carbon, Bioresour. Technol. 98 (2007) 14–21.
[36] A.W. Tan, B.H. Hameed, A.L. Ahmad, Equilibrium and kinetic studies on basic dye adsorption by oil palm fibre activated carbon, Chem. Eng. J. 127 (2007) 111–119.
[37] S.K. Behera, J.H. Kim, X. Guo, H.S. Park, Adsorption equilibrium and kinetics of polyvinyl alcohol from aqueous solution on powdered activated carbon, J. Hazard. Mater. 153 (2008) 207–1214.
[38] V. Singha, A.K. Sharmaa, D.N. Tripathia, R. Sanghib, Poly (methylmethacrylate) grafted chitosan: an efficient adsorbent for anionic azo dyes, J. Hazard. Mater. 166 (2009) 327–335.
[39] W. Ma, F.Q. Ya, M. Han, R. Wang, Characteristics of equilibrium, kinetics studies for adsorption of fluoride on magnetic-chitosan particle, J. Hazard. Mater. 143 (2007) 296–302.
[40] E. Guibal, C. Milot, O. Eterradossi, C. Gauffier, A. Domard, Study of molybdate ion sorption on chitosan gel beads by different spectrometric analyses, Int. J. Biol. Macromol. 24 (1999) 49–59.
[41] A. Ramesh, H. Hasegawa, W. Sugimoto, T. Maki, K. Ueda, Adsorption of gold (III), platinum (IV) and palladium (II) onto glycine modified crosslinked chitosan resin, Bioresour. Technol. 99 (2008) 3801–3809.
[42] J.X. Xie, Application of Infrared Spectra in Organic Chemistry and Drug Chemistry (in Chinese), Beijing Science Press, China, 2001.
[43] N. Viswanathana, C.S. Sundaramb, S. Meenakshia, Removal of fluoride from aqueous solution using protonated chitosan beads, J. Hazard. Mater. 161 (2009) 423–430.